9 Evaporite Karst in Calatayud, Iberian Chain

Francisco Gutiérrez

Abstract

The Cenozoic sedimentary fill of Calatayud Graben, an intramontane basin within the Iberian Chain, includes an evaporitic sequence around 500 m thick with significant halite and glauberite units in the subsurface. Interstratal dissolution of the salt-bearing evaporites has generated megacollapse structures covering up to 12 km^2 in which Neogene sediments have subsided as much as 200 m. The Quaternary alluvium related to the present-day fluvial systems shows sharp changes in thickness locally reaching more than 100 m. The thickened terrace deposits fill basins several kilometres long generated by dissolution-induced synsedimentary subsidence. The area offers the opportunity to examine excellent exposures of subsidence structures and paleosinkholes that illustrate the mechanisms involved in sinkhole development (sagging, collapse, and suffosion). Dissolution and hydrocompaction subsidence has caused extensive structural damage in Calatayud city, including outstanding historical buildings. On November 2003, a collapse sinkhole undermined the foundation of a five-storey building, leading to its demolition, involving around 5 million euro of direct losses.

Keywords

Subsidence • Sinkhole hazard • Salt karst • Non-tectonic deformation • Heritage loss

9.1 Introduction to the Evaporite Karst in Spain

Evaporite outcrops in Spain mostly occur in Alpine orogens and Cenozoic basins, covering more than 35,000 km^2, approximately 7 % of the total country area (Fig. 9.1). These figures explain the great diversity of evaporite karst features and the significant impact of the environmental problems related to evaporite dissolution in "Alpine Spain" (Gutiérrez et al. 2001, 2008a). Marine evaporite sedimentation covers a wide time span, from the Triassic to the present day, whereas the majority of the continental evaporites were deposited in lake environments during Paleogene and Neogene times. Most of the evaporitic formations are made up of Ca sulphate (gypsum and anhydrite) or Ca sulphate and halite. Some marine and continental formations also include K–Mg chlorides and Na sulphates (glauberite and thenardite), respectively. Geochemical and isotopic studies demonstrate that the Tertiary lacustrine evaporites were derived from the recycling (dissolution and reprecipitation) of Mesozoic marine formations (Utrilla et al. 1992). Gypsum, with an equilibrium solubility of 2.4 g/l, is commonly the only evaporitic mineral exposed at the surface. The highly soluble chloride salts and Na sulphates rarely crop out; the equilibrium solubilities of halite and glauberite ($Na_2Ca[SO_4]_2$) in distilled water are 360 and 118 g/l, respectively. However,

F. Gutiérrez (✉)
Department of Earth Sciences, University of Zaragoza, Zaragoza, Spain
e-mail: fgutier@unizar.es

F. Gutiérrez and M. Gutiérrez (eds.), *Landscapes and Landforms of Spain*, World Geomorphological Landscapes,
DOI: 10.1007/978-94-017-8628-7_9, © Springer Science+Business Media Dordrecht 2014

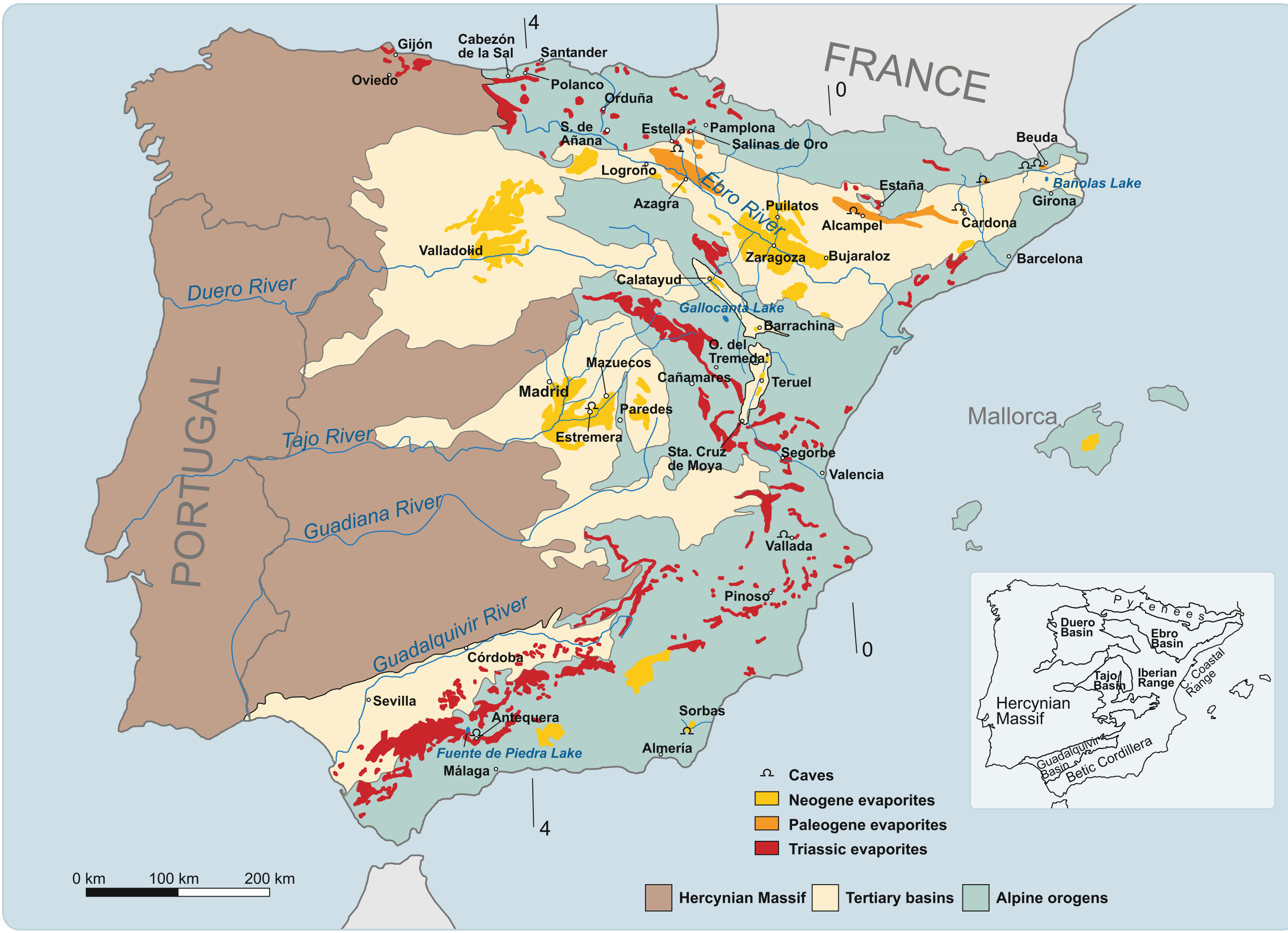

Fig. 9.1 Distribution of the main evaporite outcrops in Spain and local names of the most relevant evaporite karst areas (adapted from Gutiérrez et al. 2008a)

their dissolution by groundwater at depth, frequently unnoticed, has played an instrumental role in the development of karstic phenomena in numerous areas.

The most widespread episode of evaporitic sedimentation is recorded by Triassic shallow-marine successions up to several 100 m thick, consisting of Ca sulphate and halite units embedded in variegated marls and mudstones, mainly the Keuper facies. This formation occurs in numerous outcrops across the Alpine orogens, locally forming diapiric structures (Fig. 9.1). Evaporite karst landforms in these Triassic terrains are not frequent, most probably because the remaining salts are situated at significant depth, associated with impervious units and capped by thick karstic residues developed over long periods of time. The presence of various types of subsidence sinkholes is rather common in halokinetic structures, where groundwater flows interact with uprising salts at shallow depth: Antequera region, western Betics (Calaforra and Pulido-Bosch 1999); Pinoso Diapir, eastern Betics; Salinas de Oro, Estella, Orduña, and Polanco diapirs in the western Pyrenees. The 210-m-deep El Sumidor Cave, developed within a halokinetic structure in Vallada, eastern Betics, is one of the deepest gypsum caves in the world (Calaforra and Pulido-Bosch 1996). A relatively frequent feature in the areas underlain by the Triassic Keuper facies is the occurrence of permanent and ephemeral lakes in enclosed basins associated with either collapse sinkholes or broad subsidence depressions, including some of the largest lakes in Spain: Fuente de Piedra Lake (13.6 km^2) and the numerous lakes of Antequera area, western Betics; Gallocanta Lake (14.5 km^2), Iberian Chain (Gracia et al. 2002; Chap. 11); Estaña Lakes (López-Vicente et al. 2009), or Montcortés Lake, Pyrenees (Gutiérrez et al. 2012c). Moreover, interstratal karstification of Triassic evaporites has resulted in or contributed to the development of striking gravitational morpho-structures, including prominent fault scarps (Zenzano fault, Iberian Chain; Carbonel et al. 2013), monoclinal flexures with crestal grabens (Río Seco monocline, Iberian Chain; Gutiérrez et al. 2012a), and graben systems (grabens of Peracals, Pyrenees; Gutiérrez et al. 2012c).

The most important Tertiary marine evaporite formations from the karst perspective are (1) the halite-bearing Middle Eocene Beuda Gypsum, tectonically incorporated in the eastern sector Pyrenean orogenic wedge; (2) the Cardona Saline Formation, dominated by halite with a substantial amount of K–Mg chlorides, mainly sylvite and carnallite. This formation is exposed in the outstanding Cardona Diapir, north-eastern sector of the Ebro Basin, constituting the only significant salt outcrop (0.9 km^2) in Western Europe; and (3) the Late Messinian gypsum of the intramontane Sorbas Basin, in the eastern Betics. The Banyoles Lake is related to a cluster of coalescent collapse sinkholes generated by hypogenic dissolution of the Beuda Gypsum in a groundwater discharge zone (Canals et al. 1990). Structurally controlled sinkholes are relatively common in the alluvial surfaces developed over the Beuda Gypsum (e.g. Fluvià Valley, Sant Miquel de Camp Major), and subsidence has caused significant damage in houses of Besalú and Beuda villages. The Cardona diapir has a well-developed cave system, some of them formed in historical times in relation to anthropogenic changes induced by mining operations. The 680-m-long Forat Mico Cave is one of the longest salt caves in the world. The 335-m-long Riera Salada Cave was carved in the halite debris of a slag heap accumulated between 1925 and 1972. In March 1998, the interception of a phreatic conduit by a shallow mine led to an inrush of fresh water from the Cardener River into the underground excavations, resulting in the generation of the 4,300-m-long Salt Meanders Cave, and the development of a large number of damaging sinkholes, with the consequent abandonment of the mine (Cardona and Viver 2002; Lucha et al. 2008). The exposed salt rock, as well as the halite-rich slag heaps, displays magnificent and rapidly evolving karren and pedestals (Mottershead et al. 2008). The remarkable karst landforms developed in the Sorbas Basin are illustrated in Chap. 10.

The most significant karst features developed in Tertiary continental evaporites occur in the central sector of the Ebro Basin (Zaragoza area), Madrid Basin, and Calatayud Graben within the Iberian Chain (Gutiérrez et al. 2008a). A common characteristic of these evaporites is the presence of thick halite and glauberite units in the subsurface. The topic that has received wider attention in the Tertiary basins is the development of dissolution-induced subsidence phenomena, including sinkholes and the associated hazards. The sectors where the evaporitic bedrock is overlain by Quaternary alluvium are the most prone to subsidence. This alluvial karst occurs in reaches of the main Spanish fluvial systems where they traverse evaporitic outcrops (Fig. 9.1) and are particularly intense where the bedrock includes highly soluble salts (e.g. halite, glauberite). Commonly, in these areas, the alluvial deposits are locally thickened as much as 100 m. The thickened alluvium fills complex solution basins up to several tens of kilometres long generated by synsedimentary subsidence. Guerrero et al. (2008, 2013) present updated reviews of the alluvial systems affected by evaporite karst subsidence. Another common feature is the presence of abundant gravitational deformations that may affect the alluvial mantle (rockhead karstification), or both the cover and the bedrock (interstratal karstification). The latter is particularly common in areas where the evaporitic sequence bears halite and glauberite units in the subsurface (Guerrero et al. 2008, 2013). Interstratal dissolution of salts may also generate perched kilometre-sized enclosed depression at the valley margins that behave as starved basins (Guerrero et al. 2013). These deformation structures, together with dissolutional features found in paleokarst exposures, are the best source of information to understand the subsidence processes involved in the generation of sinkholes: sagging, suffosion, and collapse (Gutiérrez et al. 2008b). The current activity of dissolution and subsidence processes, frequently induced or accelerated by human activities, results in the formation and reactivation of sinkholes, which may constitute a geohazard of great socio-economic impact. Generally, sinkholes show a higher probability of occurrence in the lower alluvial levels, coinciding with areas where development and human activity tend to concentrate, resulting in high risk situations. The most severely affected areas include Zaragoza city and its surroundings (e.g. Galve et al. 2009; Gutiérrez et al. 2009a), Calatayud city (Gutiérrez and Cooper 2002; Gutiérrez et al. 2004), the south-eastern sector of Madrid metropolitan area, and Oviedo city. As an example, in Oviedo, dewatering for the construction of a car park induced the reactivation of an old sinkhole in 1998, resulting in the demolition of 362 apartments and direct losses estimated at 18 million euro (Pando et al. 2013).

This chapter illustrates the geological, geomorphological, and environmental implications of evaporite karst in Calatayud Graben. This is the Tertiary basin in Spain in which dissolution-induced subsidence phenomena display a wider diversity and has produced some of the most dramatic features. Here, long-sustained evaporite dissolution has generated large collapse structures in Neogene sediments, thickenings and gravitational deformation in Quaternary alluvium, and costly subsidence damage in the historical city of Calatayud.

9.2 Geological Setting

Calatayud Graben is a Cenozoic basin located within the Iberian Chain, an intraplate Alpine orogen generated by the tectonic inversion of Mesozoic extensional basins from Paleogene to Early-Middle Miocene times (orogenic stage). During the subsequent postorogenic stage, extensional tectonics has produced grabens superimposed on the previous contractional structures. A first rifting episode, which started

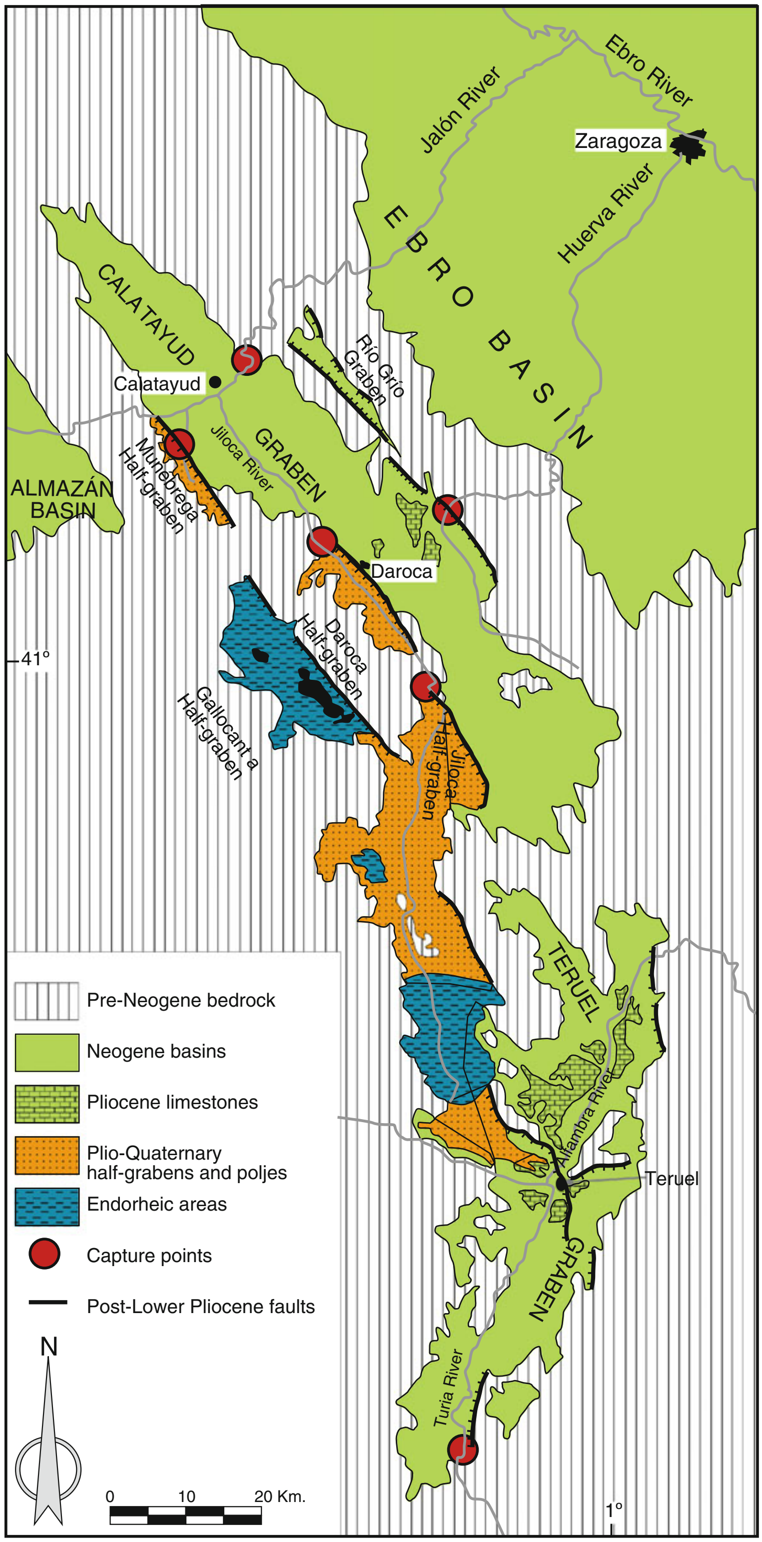

Fig. 9.2 Sketch showing the distribution of Neogene and Plio-Quaternary grabens in the central sector of the Iberian Chain

in the Lower-Middle Miocene, generated the two largest intramontane basins of the central sector of the Iberian Chain, Calatayud Graben, and Teruel Graben. Since the Late Pliocene, the second extensional episode produced new grabens locally superimposed or inset with respect to the previous basins (Gutiérrez et al. 2008c, 2012b) (Fig. 9.2).

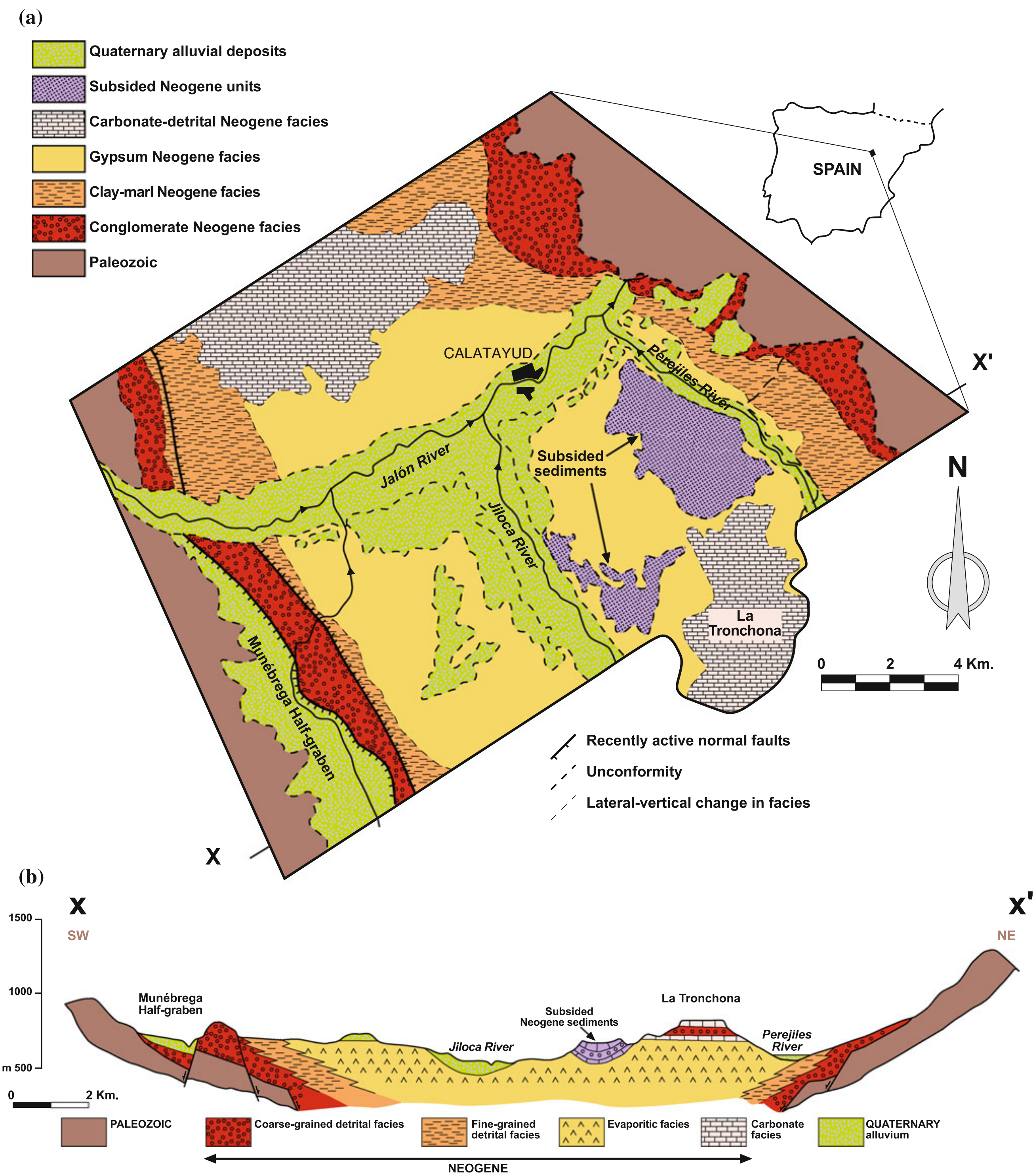

Fig. 9.3 **a** Geological sketch of a portion of Calatayud Graben in Calatayud city area, showing the facies distribution of the Cenozoic infill and the Plio-Quaternary neotectonic extensional structures developed in the south-western margin of the basin. **b** Geological cross-section across Calatayud Graben (see trace in **a**)

The change in the Neogene and Plio-Quaternary structural depressions from endorheic-aggradational to exorheic-incisional conditions has taken place through the progressive capture of the basins by the external drainage network (Fig. 9.2). Once each basin was captured, the new intra-basinal drainage incised the endorheic infill and expanded by headward erosion, developing stepped sequences of alluvial levels (pediments and terraces). This change has played an instrumental role in the development of evaporite dissolution subsidence phenomena. Under exorheic conditions, the new fluvial systems are able to evacuate large volumes of evaporites in solution, and their entrenchment leads to higher hydraulic gradients for the groundwater flows that may circulate through progressively deeper evaporite rocks (e.g. Gutiérrez et al. 2008c, 2012b).

The Calatayud Graben is a NW–SE-trending extensional basin around 110 km long and up to 25 km wide (Fig. 9.2). The age of the sedimentary fill ranges from Lower Miocene to Lower Pliocene and probably exceeds 1 km thick. In Calatayud sector, the graben is flanked by mountain ranges made up of resistant Palaeozoic rocks (Fig. 9.3). The basin fill was mainly deposited in alluvial fans distally related to lacustrine systems with evaporite and carbonate deposition. These sediments have a general subhorizontal structure and show abrupt lateral and vertical facies changes (Bomer 1960). The proximal conglomeratic facies at the margins of the graben change sharply into fine-grained clastics and evaporite–carbonate facies towards the sedimentary axis of the graben (Fig. 9.3). In the environs of Calatayud city, located close to the depocenter of the basin, the stratigraphic succession consists of the following:

- An evaporitic sequence around 500 m thick. The upper 200 m that crop out in Calatayud area is composed of laminar and nodular gypsum with thin interbedded marl partings. The gypsum ($CaSO_4 \cdot 2H_2O$) is a secondary diagenetic facies resulting from the hydration of anhydrite ($CaSO_4$) and the incongruent dissolution of glauberite (Ortí and Rosell 1998, 2000). According to Collantes and Griffo (1982), in the surroundings of Calatayud, gypsum constitutes around 85 % of the exposed evaporitic sequence. In addition to gypsum, borehole data indicate a significant proportion of halite (NaCl) and glauberite ($Na_2Ca[SO_4]_2$) at depth. The borehole described by Marín (1932) in Paracuellos de Jiloca (5 km south of Calatayud) reveals the presence of halite at depths between 170 and 537 m. Recent boreholes carried out by MYTA S. A., a few kilometres west of Calatayud, have revealed thick glauberite beds at depths higher than 15 m. Probably, the outcropping secondary gypsum is restricted to a weathered zone, grading into anhydrite, halite, and glauberite towards the unaltered inner zone of the massif, as it has been documented in the very similar Zaragoza Gypsum Formation (Salvany 2009).
- To the south of Calatayud city, the evaporite formation is overlain by a carbonate–detrital sequence around 100 m thick (Hernández et al. 1983; Sanz-Rubio et al. 2003). This succession comprises two fluvio-lacustrine limestone units with a reddish detrital unit in between (Fig. 9.3b). The upper tufaceous limestone forms the caprock of a large NW–SE-trending structural platform (La Tronchona) slightly tilted to the NW. This Late Miocene unit constitutes a useful marker to identify and assess recent deformation related to dissolution-induced subsidence and tectonics.

The sediments of the basin have been selectively excavated by the alluvial systems developed subsequently to the capture of the graben. Consequently, the topography is markedly controlled by the distribution of the different lithofacies (Bomer 1960). The conglomeratic and carbonate facies form prominent reliefs, whereas the argillaceous and evaporite sediments have been differentially eroded to form low relief areas (Fig. 9.3b). The distal carbonate sediments form the Armantes (968 m) and La Tronchona (870 m) mesas to the NW and SE of Calatayud city (533 m), respectively. The graben is transversally crossed by the Jalón River, whereas its main tributaries, the Jiloca and Perejiles rivers, have carved longitudinal valleys at both sides of La Tronchona structural platform. The evolution of these fluvial systems is recorded by stepped sequences of terraces and pediments.

During the Late Pliocene and Quaternary, Calatayud Graben area has been affected by renewed extensional block tectonics. On the western margin of the graben, NW–SE normal faults have generated the Munébrega Half-graben, superimposed to Calatayud Graben (Figs. 9.2 and 9.3). The master fault of this tectonic depression has offset a Pleistocene terrace of the Jalón River, producing an antislope scarp. A paleoseismological investigation on this fault has been conducted at this site through the excavation of a trench (Gutiérrez et al. 2009b). To the NE of Calatayud Graben, the Río Grío Graben (Fig. 9.3), traditionally interpreted as an erosional fluvial valley, corresponds to a recently discovered Plio-Quaternary graben, whose alluvial fill more than 90 m thick has been deeply incised (Gutiérrez et al. 2009c, 2012b).

9.3 Megacollapse Structures in Neogene Sediments

To the NW of La Tronchona structural platform and framed by the Jiloca and Perejiles floodplains, there are two large collapse structures in which the detrital–carbonate units stratigraphically above the evaporite sequence have subsided due to the interstratal karstification of the underlying soluble sediments (Gutiérrez 1996, 1998) (Fig. 9.3). These two zones, designated as the Maluenda and the Perejiles subsidence areas, cover 4.4 and 12 km^2, respectively (Gutiérrez 1996). Here, the supra-evaporitic subsided units are strongly deformed and locally foundered within and juxtaposed to the evaporites (Fig. 9.4). They show abundant gravitational deformation, including ductile structures

Fig. 9.4 Oblique aerial view showing strongly deformed carbonate–detrital Neogene sediments (*dark* vegetated area) foundered within the subhorizontal gypsum strata (vegetation-free light terrain) in Maluenda subsidence area

(synforms, antiforms, and flexures) with a preferential NW–SE trend and brittle structures (faults and breccias). The strike and dip of the deformed strata are very chaotic, showing sharp changes between nearby locations. In contrast, the adjacent older gypsum strata are solely affected by a joint network and maintain a subhorizontal structure. The cartographical boundary between the deformed units and the undeformed gypsum has a very irregular and interdigitated pattern (Figs. 9.3 and 9.4).

In both areas, the supra-evaporitic sediments locally show synforms and basin structures in which certain units thicken towards the core. These thickness changes have been attributed to synsedimentary dissolution-induced basins (Sanz-Rubio et al. 1997; Gutiérrez 1998). However, most of the subsidence and deformation is postsedimentary. Probably, its initiation took place once the basin became exorheic and the new drainage network started to incise the sedimentary infill. In Maluenda area, the Neogene subsided sediments are locally overlain by the deposits of a Jiloca River terrace located at 100–105 m above the channel. This alluvium, dated magnetostratigraphically as Early Pleistocene, is thickened by synsedimentary karstic subsidence, locally reaching more than 100 m in thickness. This implies that subsidence in the Neogene sediments was active before and during the sedimentation of the thickened terrace deposit (Lower Pleistocene). The fact that the floodplain deposits of the Jiloca and Perejiles rivers overlap the subsided sediments in Maluenda and Perejiles areas, respectively (Fig. 9.3), and that the deposits of a Lower Pleistocene terrace fossilize collapsed units in Maluenda area indicates that subsidence has progressed vertically downwards below the base level. Considering that the floodplains are at an altitude of 560–570 m, and that the base of the supra-evaporitic sequence is above 770 m in elevation, the maximum karst subsidence in both areas has reached at least 200 m (Gutiérrez 1996, 1998).

The intense karstification of the evaporitic formations located to the NW of the Tronchona structural platform is related to the convergence of several factors:

- The Maluenda and Perejiles subsidence areas are located in the sector where the most soluble evaporitic facies were deposited (depocenter), including a large proportion of halite and glauberite in the subsurface. Very likely, interstratal karstification has operated at several stratigraphic levels, affecting preferentially the most soluble beds.
- The NW–SE-oriented Tronchona structural platform, about 20 km long and 3 km wide, is tilted to the NW, towards the collapse areas and the main base level (Jalón River). This extensive and karstified structural surface constitutes a recharge zone, which has its main discharge area in its north-western edge, where the Maluenda and Perejiles areas are situated. This idea is supported by the presence of tufa deposits located to the NE of Paracuellos de Jiloca, which have been related to a paleospring (Gutiérrez 1996, 1998).
- The entrenchment of the fluvial systems in the sedimentary fill of the basin from the capture of the graben has favoured the circulation of underground waters through progressively deeper stratigraphic levels.
- Subsidence structures in the Neogene sediments show a prevalent NW–SE orientation. The NW–SE-trending Munébrega and Río Grío Plio-Quaternary grabens reveal

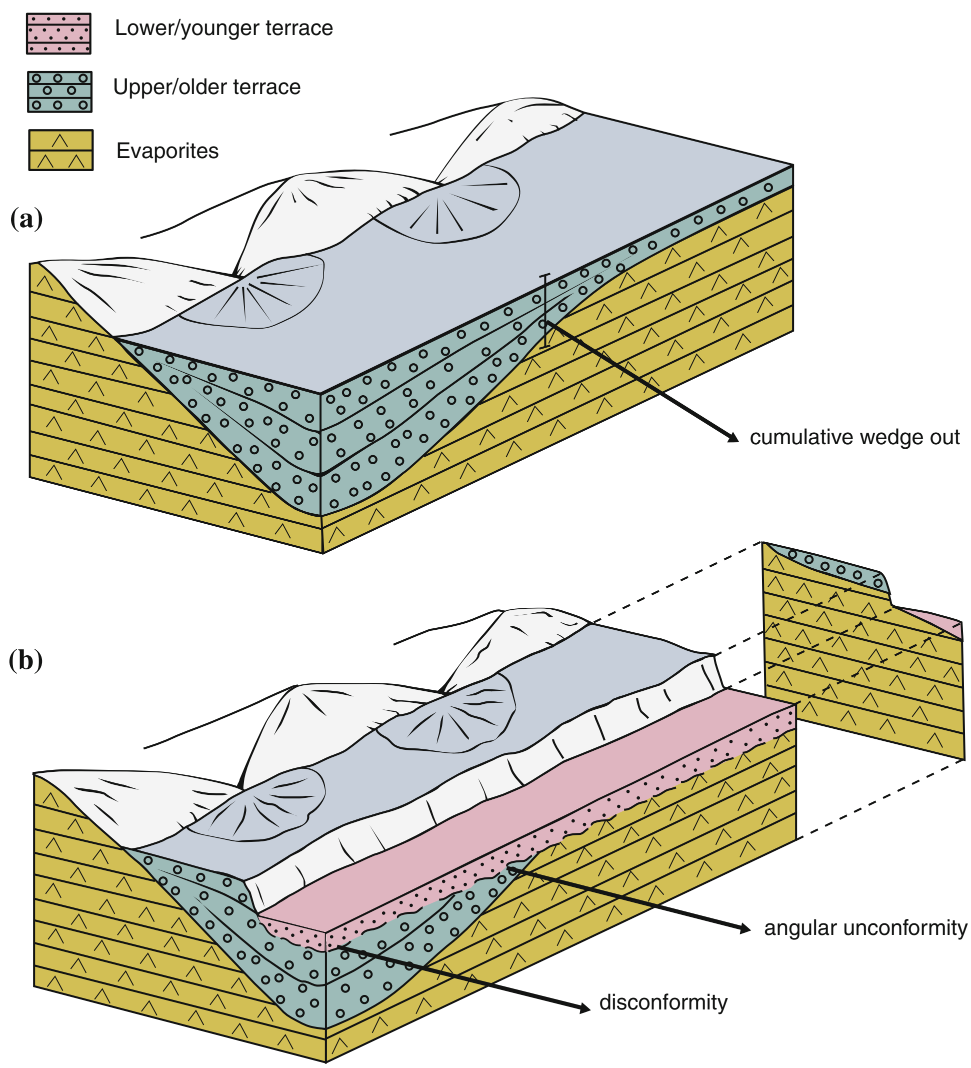

Fig. 9.5 Morpho-stratigraphic arrangement of terraces affected by synsedimentary dissolution subsidence. **a** The thickened terrace deposits fill a dissolution-induced basin showing centripetal dips and cumulative wedge-outs at the margins. **b** The deposits of the subsequent terrace are inset in the bedrock upstream of the area affected by subsidence and superposed by angular unconformity or paraconformity onto the thickened sediments of the previous alluvial level. The morphogenetic surfaces of both terraces are stepped along the whole valley reach (adapted from Gutiérrez 1998)

that the area is affected by active extensional tectonics. Probably, this extension has generated or dilated previously existing NW–SE fractures in the Neogene sediments favouring karstification along these structures. The formation and opening of fractures may be also favoured by the debutressing effect produced by the entrenchment of the Jiloca and Perejiles valleys (Jennings 1985).

- On the NE margin of the Jiloca River, in Paracuellos de Jiloca village and next to the Maluenda area, there is a spa with a perched spring that permanently issues water of the sodium chloride hydrochemical facies. This fact supports the hypothesis that karstification may be partially related to upward hypogenic groundwater flows coming from detrital aquifer units situated beneath the evaporites. Groundwater that recharges at the margins of the basin circulates through coarse-grained detrital units confined by argillaceous facies towards the axis of the basin, ultimately discharging through upward transformational flows.

9.4 Synsedimentary Subsidence and Paleosinkholes in Quaternary Alluvium

The Jalón–Jiloca–Perejiles alluvial system has been affected by synsedimentary and postsedimentary subsidence phenomena related to the karstification of the evaporitic bedrock throughout its Quaternary evolution (Gutiérrez 1996, 1998). Ten stepped alluvial levels have been differentiated within the Calatayud Graben. The height of the terrace levels above the river channels are as follows: T10: 115 m; T9: 105–100 m; T8: 90–85 m; T7: 75–70 m; T6: 65–60 m; T5: 55–50 m; T4: 45 m; T3: 35–30 m; T2: 25–20 m; T1 (floodplain): 5–3 m. Terrace levels T9 and T7 have been dated as Lower Pleistocene through magnetostratigraphic analyses. All these levels are represented by aggradation terraces. Degradation terraces developed in the deposits of older terraces (fill-cut terraces) have been recognized for some levels. The identified pediment levels are P10, P9, P8,

Fig. 9.6 Cutting of the Madrid–Zaragoza highway (A–2) next to Calatayud Hospital, showing a non-tectonic angular unconformity between dipping alluvium of terrace T8 and subhorizontal deposits of terrace T4

Fig. 9.7 Synsedimentary synform with cumulative wedge-outs affecting fine-grained terrace deposits accumulated in a palustrine area associated with a paleosinkhole (30T 612951 4577253; coordinate system ETRS89)

P7, and P4 (Px correlative to Tx). These may be aggradation surfaces (mantled pediments) or degradation surfaces developed either in older alluvium or in Miocene gypsiferous bedrock. The degradation surfaces of each level occur upstream and in the margins of the sectors where the correlative Quaternary alluvium is thickened due to synsedimentary subsidence. These spatial relationships suggest that degradation processes have been related to gradient changes in the alluvial system caused by karstic subsidence (Gutiérrez 1996, 1998).

Quaternary alluvial deposits overlying the salt-bearing evaporitic bedrock show conspicuous thickenings, recording dissolution-induced synsedimentary subsidence. Abrupt thickness variations from less than 10 m to more than 100 m may be observed in a single terrace. The thickened alluvium locally fills dissolution-induced basins with centripetal dips and cumulative wedge-outs at the margins (Fig. 9.5). These thickened terrace deposits show a high proportion of flood-plain facies, whereas in areas where the alluvium has not been affected by synsedimentary subsidence, channel gravel facies dominate. As a consequence of the local thickening of the alluvium, the deposits of a younger terrace may be inset into the bedrock or superposed onto older thickened and deformed deposits. Nonetheless, the surfaces of both terraces may show a stepped arrangement along the whole valley reach (Fig. 9.5). These morpho-stratigraphic features, very common in fluvial valleys carved in Tertiary evaporites in Spain, can be observed on the eastern margin of the Jiloca River valley, next to the confluence with the Jalón River. Here, the deposits of several terraces fill a dissolution-induced

Fig. 9.8 Dissolution and subsidence structures exposed in cuttings of the Madrid–Zaragoza highway (A–2) along the southern margin of Jalón Valley. **a** Sagging in terrace deposits related to the dissolutional lowering of the evaporite rockhead. Note the marly karstic residue between the bedrock and the cover. **b** Dissolutional conduits filled with alluvium derived from the overlying terrace deposits. **c** Sagging and collapse on bedrock related to deep-seated interstratal karstification. The collapse structure is controlled by outward-dipping antithetic normal faults and brecciation. **d** Collapse structure with dome-shaped failure surfaces related to the upward propagation (stoping) of a deep-seated cavity

trough more than 4 km long and 0.7 km wide where the alluvium thickness exceeds 100 m. The southern cutting of the A-2 Madrid–Zaragoza motorway next to N-234 road shows the superposition of two sedimentary units bounded by angular unconformity (Fig. 9.6). The thickened and deformed deposits of the lower unit have been ascribed to the Early Pleistocene terrace level T8 (90–85 m above the channel). The deposits of this terrace reach more than 90 m in vertical thickness (the stratigraphic thickness is higher), and its 25° dip progressively attenuates towards the top of the sequence. The upper unit corresponds to terrace T4 (45 m above the channel). The deposits of this terrace, capped by a petrocalcic horizon, show a progressive thickness increase towards the NE, and its aggradation surface is tilted in the same direction, indicating that the terrace has undergone long-sustained synsedimentary and postsedimentary dissolution-induced subsidence.

The alluvial cover overlying the evaporite bedrock shows numerous ductile and brittle gravitational deformation structures (Hoyos et al. 1977; Gutiérrez 1996, 1998). Some of these dissolution-induced deformations also affect the evaporitic bedrock (interstratal karstification). Excellent examples are found in the cuttings of the A-2 Zaragoza–Calatayud motorway, along the southern margin of the Jalón Valley. Many of these subsidence structures correspond to paleodolines that were filled with marl and carbonate palustrine–lacustrine facies, recording the development of swampy environments and ponds in closed depressions in the floodplain. Remains of aquatic gastropods, amphibian, and fishes have been found in some of these paleosinkhole fills (Fig. 9.7). These structures and the associated sediments provide valuable information on the subsurface processes involved in the currently active subsidence. Four main mechanisms of sinkhole generation have been identified through the study of the subsidence structures identified in the exposed paleokarst (Gutiérrez et al. 2008b; Gutiérrez and Cooper 2013) (Fig. 9.8): (a) progressive lowering of the evaporitic rockhead by dissolution and gradual sagging of the alluvial cover (cover sagging sinkholes) (Fig. 9.8a); (b) development of dissolutional conduits and fissures (grikes) at the top the bedrock and downward migration (ravelling) of detrital particles from the alluvial cover (Fig. 9.8b); this process may cause the progressive settlement of the alluvial mantle (cover suffosion sinkholes), or the upward propagation of cavities through cohesive alluvium that may eventually produce catastrophic collapses (cover collapse sinkholes); (c) sheet-like dissolution within the evaporitic bedrock, typically focused on salt beds, and progressive sagging of the overlying bedrock and alluvial cover (bedrock and cover sagging sinkholes) (Fig. 9.8c); (d) generation of dissolutional cavities within the bedrock and upward propagation of the void by progressive roof collapse (stoping), culminating in the formation of bedrock collapse sinkholes and bedrock and cover collapse sinkholes (Fig. 9.8c and d).

One of the best examples of a paleosinkhole may be examined in a gravel pit excavated in the T4 terrace NW of Calatayud Hospital (30T 612951 4577253; coordinate system ETRS89). The paleosinkhole displays several superimposed ductile and brittle subsidence structures, as well as soft-sediment deformation, whose relative chronology may be inferred on the basis of cross-cutting relationships (Fig. 9.7): (a) Synform in section and basin structure in 3D made up of marls and fines deposited in a ponded and/or swampy doline developed by bending in the floodplain. The thickening of the strata towards the core and the upward dip attenuation (cumulative wedge-out) indicate that subsidence was coeval to deposition. (b) The sagging structure is crosscut by subvertical normal faults (ring faults) recording the development of a collapse sinkhole. Ductile structures and soft-sediment deformation associated with these failure planes suggest that the collapse occurred during or soon after deposition, when the alluvium was still in a soft and water-saturated state. This temporal evolution pattern has relevant applied implications, revealing that slow subsidence in a sinkhole may eventually transform into more dangerous catastrophic collapse. Soft-sediment deformation includes irregular masses of gravel (gravel pockets) embedded in fine-grained facies, spatially associated with the collapse faults. Similar structures have been interpreted by several authors as liquefaction–fluidization features (Postma 1983; Johnson 1986; Nocita 1988). These gravel pockets may be explained as liquefaction structures caused by local sediment shaking and fluid overpressure induced by the generation of a catastrophic sinkhole (Gutiérrez 1998).

Fig. 9.9 Tilted tower (11th–12th C) of San Pedro de los Francos Church (14th C) in La Rúa Street. The *upper* 5-m-high portion of the tower was removed in 1840 to avoid its collapse over the Wersage Palace located in the opposite side of the street, where the Royal family used to be hosted

9.5 Subsidence Hazard in Calatayud Historical City

Calatayud city was founded by the Muslims in 716 AD at an important junction of communication routes. In 1120 AD, it was conquered by King Alfonso I "the Battler". This attractive city from the historical and artistic point of view was declared Historical Monument in 1967 and currently has a population of around 22,000 inhabitants. Although the urban area is located in an advantageous location from the economic perspective, its geomorphological setting has posed severe problems since old times. The city is located on the NW margin of the Jalón River valley (Fig. 9.3), at the foot of a nearly vertical gypsum escarpment approximately 100 m high. It is positioned partly on an alluvial fan fed by La Rúa and Las Pozas streams and partly on the Jalón River floodplain. The city also extends onto the gypsum cliff, with cave dwellings excavated in the slopes. Since its foundation, urban development has been largely constrained by geohazards, including (a) floods caused by the Jalón River, and La Rúa and Las Pozas streams, which have caused severe damage in the floodplain and the alluvial fan, respectively. Run-off of the flashy La Rúa and Las Pozas streams has been progressively diverted through the construction of dams, artificial channels, and tunnels since Muslim times

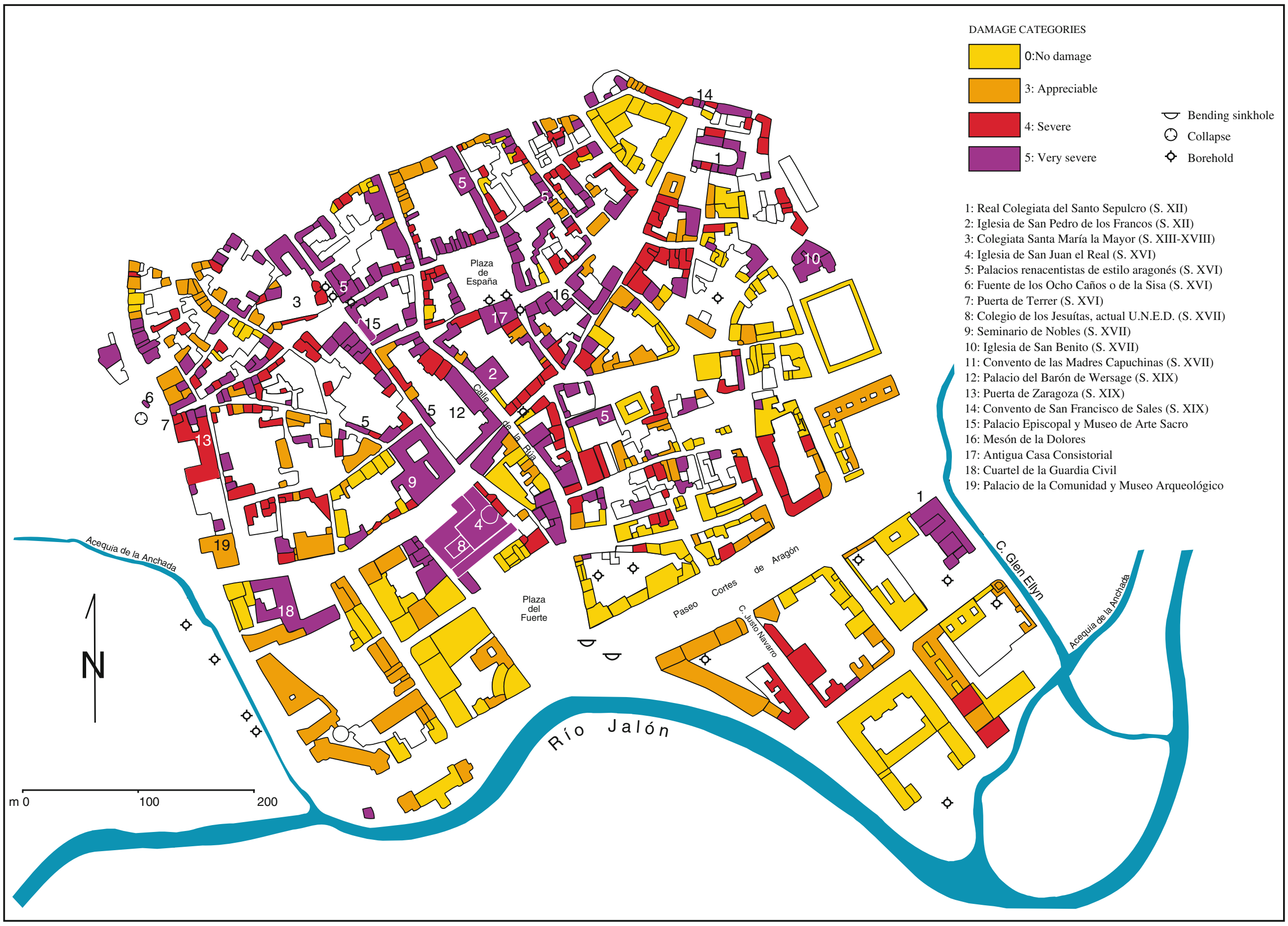

Fig. 9.10 Map showing the distribution of subsidence damage in a sector of Calatayud city (modified from Gutiérrez 1998). The *green asterisk* indicates the location of the Blue House, undermined by a collapse sinkhole in 10 November 2003

(see Gutiérrez and Cooper 2002); (b) rockfalls and topples have constrained development on the gypsum scarp areas. In 1988, a person was killed by a rockfall. These rapid slope movements have caused the destruction of several buildings and frequent cuts in the roads running along the foot of the cliff; (c) subsidence causes severe detrimental effects on both the floodplain and fan areas.

Most of the old buildings in the city have been damaged by subsidence, and some important monuments have been demolished. Calatayud is considered from a geotechnical perspective the most problematic city of Aragón Region, both for remediation of historical buildings and for modern development. Subsidence damage in the buildings includes tilting and cracking (Fig. 9.9), sloping floors, sheared door and window openings, and collapsed roofs. Peripheral damage includes broken pipes, with the consequent extra water supply to the subsurface, and pavement sagging and collapse. The full cost of the damage is difficult to estimate, but the losses to the irreplaceable artistic and historical heritage are large. The spatial distribution of the subsidence and its causes have been analysed on the basis of the geotechnical characterization of the materials beneath Calatayud and a systematic building damage assessment (Gutiérrez 1998; Gutiérrez et al. 2000; Gutiérrez and Cooper 2002).

The stratigraphic and geotechnical characteristics of the rocks and soils beneath Calatayud city were studied from 43 boreholes, 18 of which reached the evaporitic bedrock. From the surface downwards, these materials include the following:

- A top layer of unsorted and unconsolidated anthropogenic ground whose thickness decreases towards the Jalón River. Compaction of the made-ground rubble may locally affect buildings resting directly on the fill.
- Alluvial fan deposits mainly consisting of gypsiferous silts with scattered gypsum and limestone clasts. This unit is more than 12 m thick in the proximal fan area and wedges out towards the floodplain. These soils are characterized by a very loose packing with the silt particles bound by gypsum "bridges". This deposit may undergo a rapid reduction in volume with the addition of water due to dissolution of the interparticle gypsum bonds and the consequent collapse of the granular framework

(hydrocollapse or hydrocompaction). This type of subsidence may affect structures in the fan area.

- Fluvial deposits underlie the gypsiferous silts in the fan area and the made-ground in the floodplain. In the floodplain area, the thickness of these deposits ranges from 7 to 24 m. The thickness variations are largely related to synsedimentary subsidence phenomena. They are made up of channel gravels and floodplain fines, including palustrine facies deposited in swampy subsidence depressions that locally reach more than 6 m in thickness. The consolidation of these deposits may cause subtle settlement of the ground surface.
- A karstic residue up to 9 m thick, composed of soft, dark grey marls with scattered gypsum particles between the alluvium and the evaporitic bedrock.
- The karstic residue grades downwards into the evaporitic bedrock with a well-developed tertiary porosity (solutionally enlarged discontinuity planes).

The spatial distribution and intensity of the subsidence were indirectly analysed through the construction of a building damage map of a broad sector of the city covering around 35 ha (Fig. 9.10). The selected area includes buildings varying in age from twelfth century to modern and includes a wide range of morpho-stratigraphic settings, from the proximal fan area to the riverbank. The damage was assessed in 1996–1997 by examination of the building façades. A damage category was assigned to each building on a scale of 0–5, based on the *Subsidence Engineers' Handbook* ranking system established by the British National Coal Board (NCB) for the evaluation of mining subsidence damage (NCB 1975). Peripheral effects and internal damage of the buildings were not surveyed in the study, so only four levels of damage 0, 3, 4, and 5 were used. Thus, level 0 on the map also includes damage attributable to levels 1 and 2 in the NCB ranking. Although this methodology has clear limitations, mainly because of the heterogeneity of the "structural markers", the damage map provides a rough idea about the distribution of the subsidence effects and allows inferring the main causative processes.

The map of the subsidence categories shows that buildings affected by severe damage (level 5) are found in all the sectors of the selected area (Fig. 9.10). However, the proximal fan area has a higher concentration of buildings with the highest damage category. In this area, the blocks flanking La Rúa Street are the most severely affected. The presence of buildings affected by severe damage throughout the whole study area, including sites without anthropogenic rubble or gypsiferous silts, indicates that karstification of the bedrock is one of the main causes of the subsidence. The relatively greater impact of subsidence in the proximal fan area suggests that hydrocollapse and possibly dissolution of the gypsiferous silts contribute significantly to subsidence in this area. The higher subsidence activity in La Rúa Street may be explained by the high thickness of the anthropogenic rubble and the existence of preferential underground flows along the buried La Rúa channel (Fig. 9.9). Other processes, such as compaction of man-made ground, consolidation of fluvial deposits, or the collapse of old cellars, may also play a relevant role at specific sites, but do not seem to contribute significantly to the subsidence that affects a great part of the urban area. Additional information on subsidence damage and remediation history of some remarkable historical buildings (e.g. Santa María la Mayor, San Pedro de los Francos Church, Spain Square, Ocho Caños Fountain) may be found in Gutiérrez and Cooper (2002).

Fig. 9.11 Collapse sinkhole occurred catastrophically in 10 November 2003 next to and beneath the *Blue* House. *Photograph* taken in the morning of November 10

To our knowledge, the most infamous subsidence event occurred in Calatayud corresponds to the 2003 collapse sinkhole that led to the demolition of the so-called Blue House (Fig. 9.11). This was a five-storey building with basement built in the 1970s on the Jalón River floodplain (location indicated with an asterisk in Fig. 9.10). On the night of 9 November 2003, some of the tenants of the 52 flats perceived strange noises and the occurrence of cracks. At around 3:30 a.m., subsequent to the evacuation of the building, a sinkhole 6 m long formed suddenly and noisily in the pavement next to the Blue House (Fig. 9.11). The water table, located at a depth of 3 m, made it impossible observing the bottom of the depression. On the morning of November 10, the sinkhole started to be filled with gravel to prevent the widening of the hollow by mass wasting processes. After dumping 350 m^3 of aggregate, a volume much greater than the expected, the technical party of the City Council suspected that the cavity could extend underneath the basement of the building. This hypothesis was corroborated by means of perforations conducted in the basement; they detected a funnel-shaped cavity with a 10-m-deep apex located beneath the Blue House. An additional 250 m^3 of concrete was needed to fill the void. A cavity, rooted in the cavernous bedrock, propagated upwards through the alluvial cover by progressive roof collapse. Once it reached the rigid base of the building and the pavement, it enlarged laterally generating a funnel-shaped void. Undermining of the foundations of the building caused the brittle deformation of the structure. Subsequently, a portion of the pavement bridging the cavity failed, resulting in the observed collapse sinkhole (Gutiérrez et al. 2004). In subsequent days, intense geotechnical investigations and stabilization works were carried out. A few months later, the Blue House was demolished. Considering estimated costs of 3 million euro for the flats, 1 million for the stabilization works and geotechnical investigations, and 0.8 million for the demolition, the direct economic losses caused by this unforeseeable single subsidence event exceed 4.8 million euros. Additional costs have been derived from housing rentals, the closure of businesses, moves, and land depreciation (Gutiérrez et al. 2004). The owners demanded a compensation to the *Consorcio de Compensación de Seguros* (a consortium integrated and funded by all insurance companies), which covers losses related to extraordinary events like some geohazards or terrorist attacks. Unfortunately, this institution does not cover sinkhole-related damage, heading the owners to a state of neglect; mortgages of non-existing flats are being paid.

Acknowledgments This work has been supported by the Spanish national project CGL2010-16775 (Ministerio de Ciencia e Innovación and FEDER) and the regional project 2012/GA-LC-021 (DGA-La Caixa).

References

Bomer B (1960) Aspectos morfológicos de la Cuenca de Calatayud-Daroca y de sus zonas marginales. Estudios Geográficos 80:393–402

Calaforra JM, Pulido-Bosch A (1996) Some examples of gypsum karst and the most important gypsum caves in Spain. Int J Speleol 25:225–237

Calaforra JM, Pulido-Bosch A (1999) Gypsum karst features as evidence of diapiric processes in the Betic Cordillera, Southern Spain. Geomorphology 29:251–264

Canals M, Got H, Juliá R, Serra J (1990) Solution-collapse depressions and suspensates in the limnocrenic lake of Banyoles (NE Spain). Earth Surf Proc Land 15:243–254

Carbonel D, Gutiérrez F, Linares R, Roqué C, Zarroca M, McCalpin J, Guerrero J, Rodríguez V (2013) Differentiating between gravitational and tectonic faults by means of geomorphological mapping, trenching and geophysical surveys. The case of the Zenzano fault (Iberian Chain, N Spain). Geomorphology 189:93–108

Cardona F, Viver J (2002) Sota la Sal de Cardona. Espeleo Club de Gràcia, Barcelona 129 p

Collantes LP, Griffo JL (1982) Panorámica general del yeso en España. Los yesos de la Cubeta de Calatayud en la Provincia de Zaragoza. Tecniterrae 8(46):53–63

Galve JP, Gutiérrez F, Lucha P, Bonachea J, Remondo J, Cendrero A, Gutiérrez M, Gimeno MJ, Pardo G, Sánchez JA (2009) Sinkholes in the salt-bearing evaporite karst of the Ebro River valley upstream of Zaragoza city (NE Spain). Geomorphological mapping and analysis as a basis for risk management. Geomorphology 108:145–158

Gracia FJ, Gutiérrez F, Gutiérrez M (2002) Origin and evolution of the Gallocanta polje (Iberian Range, NE Spain). Zeitschrift für Geomorphology 46:245–262

Guerrero J, Gutiérrez F, Lucha P (2008) The impact of halite dissolution subsidence on fluvial terrace development. The case study of the Huerva River in the Ebro Basin (NE Spain). Geomorphology 100:164–179

Guerrero J, Gutiérrez F, Galve JP (2013) Large depressions, thickened terraces, and gravitational deformation in the Ebro River valley (Zaragoza area, NE Spain): evidence of glauberite and halite interstratal karstification. Geomorphology 196:162–176

Gutiérrez F (1996) Gypsum karstification induced subsidence: effects on alluvial systems and derived geohazards (Calatayud Graben, Iberian Range, Spain). Geomorphology 16:277–293

Gutiérrez F (1998) Fenómenos de subsidencia por disolución de formaciones evaporíticas en las fosas neógenas de Teruel y Calatayud. Ph. D. thesis, University of Zaragoza, 569 p

Gutiérrez F, Cooper AH (2002) Evaporite dissolution subsidence in the historical city of Calatayud, Spain: damage appraisal and prevention. Nat Hazards 25:259–288

Gutiérrez F, Cooper AH (2013) Surface morphology of gypsum karst. In: Frumkin A (ed) Treatise on geomorphology. Karst Geomorphology, vol 6. Elsevier, Amsterdam, pp 425–437

Gutiérrez F, Cooper AH, García-Hermoso F (2000) Spatial assessment, mitigation and prevention of evaporite dissolution subsidence damage in the historical city of Calatayud, Spain. In: Carbognin L, Gambolati G, Johnson AI (eds) Land subsidence. Proceedings of the 6th international symposium on land subsidence, vol 1, pp 237–248

Gutiérrez F, Ortí F, Gutiérrez-Elorza M, Pérez-González A, Benito G, Gracia-Prieto J, Durán JJ (2001) The stratigraphical record and activity of evaporite dissolution subsidence in Spain. Carbonates Evaporites 16:46–70

Gutiérrez F, Lucha P, Guerrero J (2004) La dolina de colapso de la casa azul de Calatayud (noviembre de 2003). Origen, efectos y pronóstico. In: Benito G, Díez-Herrero A (eds) Riesgos naturales y antrópicos en Geomorfología. Actas de la VIII Reunión Nacional de Geomorfología, Toledo, pp 477–488

Gutiérrez F, Calaforra JM, Cardona F, Ortí F, Durán JJ, Garay P (2008a) Geological and environmental implications of evaporite karst in Spain. Environ Geol 53:951–965

Gutiérrez F, Guerrero J, Lucha P (2008b) A genetic classification of sinkholes based on the analysis of evaporite paleokarst exposures in Spain. Environ Geol 53:993–1006

Gutiérrez F, Gutiérrez M, Gracia FJ, McCalpin JP, Lucha P, Guerrero J (2008c) Plio-Quaternary extensional seismotectonics and drainage network development in the central sector of the Iberian range (NE Spain). Geomorphology 102:21–42

Gutiérrez F, Galve JP, Lucha P, Bonachea J, Jordá L, Jordá R (2009a) Investigation of a large collapse sinkhole affecting a multi-storey building by means of geophysics and the trenching technique (Zaragoza city, NE Spain). Environ Geol 58:1107–1122

Gutiérrez F, Masana E, González A, Guerrero J, Lucha P, McCalpin JP (2009b) Late Quaternary paleoseismic evidence on the Munébrega half-graben fault (Iberian range, Spain). Int J Earth Sci 98:1691–1703

Gutiérrez F, Lucha P, Jordá L (2009c) The Río Grío depression (Iberian Range, NE Spain). Neotectonic graben vs. fluvial valley. In: Pérez-López R, Grützner C, Lario J, Reicherter K Silva P (eds) Archeoseismology and palaeoseismology in the Alpine-Himalayan collisional zone. 1st INQUA-IGCP-567 international workshop on earthquake archaeology and palaeoseismology, Baelo Claudia, Spain, pp 43–46

Gutiérrez F, Carbonel D, Guerrero J, McCalpin JP, Linares R, Roque C, Zarroca M (2012a) Late Holocene episodic displacement on fault scarps related to interstratal dissolution of evaporites (Teruel Neogene Graben, NE Spain). J Struct Geol 34:2–19

Gutiérrez F, Gracia FJ, Gutiérrez M, Lucha P, Guerrero J, Carbonel D, Galve JP (2012b) A review on Quaternary tectonic and nontectonic faults in the central sector of the Iberian Chain, NE Spain. J Iberian Geol 38:145–160

Gutiérrez F, Linares R, Roqué C, Zarroca M, Rosell J, Galve JP, Carbonell D (2012c) Investigating gravitational grabens related to lateral spreading and evaporite dissolution subsidence by means of detailed mapping, trenching, and electrical resistivity tomography (Spanish Pyrenees). Lithosphere 4:331–353

Hernández A, Del Olmo P, Aragonés E (1983) Memoria y Mapa Geológico de España, E. 1:50.000. Ateca (437). IGME, Madrid

Hoyos M, Zazo C, Goy JL, Aguirre E (1977) Estudio geomorfológico en los alrededores de Calatayud. Actas de la III Reunión Nacional de Cuaternario Ibérico, pp 149–160

Jennings JN (1985) Karst geomorphology. Blackwell, Oxford 239 p

Johnson SY (1986) Water-escape structures in coarse-grained, volcaniclastic, fluvial deposits of the Ellensburg formation, South-Central Washington. J Sediment Petrol 56(6):905–910

López-Vicente M, Navas A, Machín J (2009) Geomorphic mapping in endorheic catchments in the Spanish Pyrenees: an integrated GIS analysis of karstic features. Geomorphology 111:38–47

Lucha P, Cardona F, Gutiérrez F, Guerrero J (2008) Natural and human-induced dissolution and subsidence processes in the salt outcrop of the Cardona Diapir (NE Spain). Environ Geol 53:1023–1035

Marín A (1932) Boletín de Sondeos. IGME, Madrid 3(1):29–99

Mottershead DN, Duane WJ, Inkpen RJ, Wright JS (2008) An investigation of the geometric controls on the morphological evolution of small-scale salt terrains, Cardona, Spain. Environ Geol 53:1091–1098

NCB (1975) Subsidence engineers' handbook. National Coal Board Mining Department, United Kingdom 111 p

Nocita BW (1988) Soft-sediment deformation (fluid escape) features in a coarse-grained pyroclastic-surge deposit, north-central New Mexico. Sedimentology 35:275–285

Ortí F, Rosell L (1998) Unidades evaporíticas de la Cuenca de Calatayud (Mioceno inferior-medio, Zaragoza). Geogaceta 23:111–114

Ortí F, Rosell L (2000) Evaporite systems and diagenetic patterns in the Calatayud basin (Miocene, Central Spain). Sedimentology 47:665–685

Pando L, Pulgar JA, Gutiérrez-Claverol M (2013) A case of man-induced ground subsidence and building settlement related to karstified gypsum (Oviedo, NW Spain). Environ Earth Sci 68:507–519

Postma G (1983) Water escape structures in the context of a depositional model of a mass flow dominated conglomeratic fan-delta (Abrioja Formation, Pliocene, Almería Basin, Spain). Sedimentology 30:91–103

Salvany JM (2009) Geología del yacimiento glauberítico de Montes de Torrero. Universidad de Zaragoza, Zaragoza 80 p

Sanz-Rubio E, Hoyos M, Calvo JP, Sánchez-Moral S, Cañaveras JC, Sesé C (1997) Paleokarstificaciones y evolución de los sistemas deposicionales miocenos de la Cuenca de Calatayud. In: Alcalá L, Alonso-Zarza AM (eds) Itinerarios Geológicos en el Terciario del Centro y Este de la Península.). Excursiones del III Congreso del Grupo Español del Terciario, Cuenca, pp 109–134

Sanz-Rubio E, Sánchez-Moral S, Cañaveras JC, Abdul-Aziz H, Calvo JP, Cuezva S, Mazo AV, Rouchy JM, Sesé C, van Dam J (2003) Síntesis de la cronoestratigrafía y evolución sedimentaria de los sistemas lacustres evaporíticos y carbonatados neógenos de la cuenca de Calatayud-Montalbán. Estud Geol 59:83–105

Utrilla R, Pierre C, Ortí F, Pueyo JJ (1992) Oxygen and sulphur isotope compositions as indicators of the origin of Mesozoic and Cenozoic evaporites from Spain. Chem Geol (Isotope Geoscience Section) 102:229–244